

Biomass Pyrolysis of *Helianthus annuus* Stems: Qualitative and Quantitative Study Based on Py-GC/MS

Fu-Xin Chen,^a Pin Gong,^b Hui-Kuan Zhang,^a Xiao-Huan Bai,^b Yong-Fei Gao,^a and An-Ning Zhou^{a,*}

The pyrolytic product vapor of *Helianthus annuus* stems was analyzed by Pyrolysis–gas chromatography–mass spectrometry (Py-GC/MS) using the internal standard (ISTD) method with different pyrolysis temperatures and times. 1,3,5-tri-tert-butylbenzene (TTBB) was found to be the best ISTD chemical in this study. Scanning electron microscopy (SEM) revealed that, for the solid-state product, the pores and mesh structure gradually increased along with the pyrolysis temperatures and time. Sintering and porous destruction were observed at a lower pyrolysis temperature (600 °C) with longer time (0.5 min). The pyrolysis vapors contained small gas molecules such as CO₂ as well as complex organic compounds, mainly alcohols, esters, acids, aldehydes, ketones, aromatic compounds, etc. In these products, aldehyde, ketone, and aromatic compounds were the main biochemicals; the appropriate pyrolysis temperature to produce aldehydes and ketones was 700 °C, and 600 °C was suitable for aromatic compounds. The regularity of the distribution of products and pyrolytic conditions was explored through eight representative compounds. The relationship between the product contents and pyrolysis conditions were complex for *Helianthus annuus* stems, but partial least squares discriminant analysis (PLS-DA) methods were a powerful tool for screening biochemicals whose absolute contents were sensitive to the pyrolysis conditions.

Keywords: *Helianthus annuus* stems; Py-GC/MS; ISTD; Absolute content; PLS-DA

Contact information: a: School of Chemistry and Chemical Engineering, Xi'an University of Science and Technology, Xi'an, 710054, China; b: College of Life Science and Technology, Shaanxi University of Science and Technology, Xi'an, 710021, China; *Corresponding author: chenfuxin1981@163.com

INTRODUCTION

Biomass is a potential source of renewable energy and chemicals that can be utilized sustainably (Gopalan *et al.* 2015; Nielsen *et al.* 2016). The new generation of biomass per year is about 170 billion tons, converted into 85 billion ton standard coal or 60 billion ton oil equivalent; this amount represents about five times the global total primary energy supply in 2007. *Helianthus annuus*, as an annual herbaceous crops acreage, has reached 1.18 million hectares just in China (Alexander and Schrag 2003). One of the important ways that biomass can be converted to bio-oil or biochemicals is through fast pyrolysis (Bridgwater and Peacocke 2000). The fast pyrolysis of biomass to product biochemicals has attracted on-going attention in the research and development of renewable biomass resources due to its characteristics, such as its low cost, easy operability, and its ability to retain a maximum of its useful chemical structure, etc. (Mohan *et al.* 2006).

Compared with petroleum-derived chemicals, biochemicals have a more complex mixture, as they can consist of hundreds of organic compounds with different functional groups, including alcohols, acids, aldehydes, esters, ketones, phenols, alkanes, *etc.* Many of them are important raw materials in the fine chemicals industry, so they are also called an “inexhaustible fine chemicals plant” (Zhou *et al.* 2011).

Compared with other biomass, such as wood (Wang *et al.* 2015), peanut shells (Ahmad *et al.* 2012), rice husks (Zhang *et al.* 2016), and bamboo (Yan *et al.* 2016), *Helianthus annuus* stems have much higher acreage and annual outputs, and the distribution, pyrolysis process, and pyrolysis product of *Helianthus annuus* stems are different than those of woody plants. The large variety of renewable characteristics and the distribution of different products prompted this research on the use of new approaches in pyrolysis instead of direct combustion.

Because of the complex mixture and the low content of any single component, it is difficult to synchronously make qualitative and quantitative analysis of biochemicals, although both are key for researchers to clarify mechanisms of processes and industrial application (Sun *et al.* 2010). To address this difficulty, many analysis methods have been developed in recent years, such as gas chromatography (GC) (Silva *et al.* 2014), gas chromatography–mass spectrometry (GC-MS) (Butler *et al.* 2013), gas chromatography–Fourier Transform Infrared Spectroscopy (GC-FTIR) (Shen *et al.* 2010), liquid chromatography–mass spectrometry (LC-MS) (Mullen *et al.* 2010), elemental analysis (Naik *et al.* 2010), and nuclear magnetic resonance (NMR) spectroscopy (Falco *et al.* 2011). In these methods, pyrolysis-gas chromatography/mass spectrometry (Py-GC/MS) methods were used widely for the powerful separation capabilities and relatively easy qualitative analysis of the pyrolysis vapors (Lu *et al.* 2011). In previous research, it was found that it was not enough to merely study relative content (Zhang *et al.* 2013). One obvious reason was that a considerable part of the pyrolysis product, for example, char and char-analog chemicals, could not be detected by GC and any GC coupling instrument (Meng *et al.* 2016). This study researches the solid product structure by scanning electron microscopy (SEM) and the absolute content of pyrolysis vapor by an internal standard method (ISTD).

A few experiments have reported in off-line pyrolysis research in which the internal standard was added to the solution of pyrolysis and injected in the gas chromatograph (Zhang *et al.* 2012). These two separate processes were useful for the off-line pyrolysis coupling with the GC-MS analysis methods. Many chemicals have been scanned and selected for ISTD, such as margaric acid methyl ester (Jabeur *et al.* 2015), nonadecane acid methyl ester (Rostad and Pereira 1986), 1-tridecanol (Choi and Oh 2014), cholesterol (Görög and Chafetz 1980), *etc.*, depending on the experiment’s requirements. However, few of these chemicals can be used in on-line pyrolysis because the operating temperature in the pyrolysis oven is much higher than the GC-MS temperature. Thermal stability is the first consideration for the on-line PY-GC/MS. Some commercially available chemicals used in the GC-MS experiment were tested in the pyrolysis of *Helianthus annuus* stems by PY-GC/MS; unfortunately, all of them decomposed at pyrolysis temperature. In order to research the pyrolysis of *Helianthus annuus* stems through the accurate calculation of product contents and to thoroughly understand the pyrolysis process and mechanism (Aysu *et al.* 2016), a new ISTD chemical needs to be developed to analyze the products more accurately and comprehensively.

EXPERIMENTAL DETAILS

Material

Helianthus annuus stems used in this study were picked from Shenmu County, Shaanxi, China. After 2 h of drying under 80 °C drum wind, samples were smashed using a DF-70 high-speed continuous feed mill (Gongyi, China), grinding and sieved with 80 mesh sieve, then sealed and stored until use (Kleen *et al.* 1993).

Table 1. Industrial and Elemental Analysis of *Helianthus annuus* Stems

Analyses of <i>Helianthus annuus</i> stems (%)				Elemental analysis (%)				
M _{ad}	A _{ad}	V _{ad}	FC _{ad} *	C	H	N	S	O*
5.62	3.63	84.22	6.53	48.35	4.86	0.16	0.34	46.29

*Calculated by subtraction

As shown in Table 1, after they were dried, *Helianthus annuus* stems had little moisture (5.62%) and ash (3.63%), and were mostly volatile (84.22%) except for fixed carbon (6.53%). They also had a higher content of hydrogen (4.86%) and a lower content of carbon (48.35%) compared with oils or coals. Compared with other ligneous plants, *Helianthus annuus* stems also had a lower carbon content and higher hydrogen and oxygen content (Chen *et al.* 2011). These compositions were more conducive to the production of hydrogen-rich and oxygen-rich compounds in fast pyrolysis.

Methods

TG/DTG analytical methods

Thermogravimetric analysis (TG) and differential thermal analysis (DTA) were performed with a Mettler-Toledo TGA-DSC1 HT thermal analyzer (Zurich, Switzerland). Samples of 5.0000 mg were analyzed in an Al₂O₃ crucible at heating rates of 5, 10, and 20 K/min from room temperature to 1073 K in an atmosphere of nitrogen (99.999%) flowing at 30 mL/min.

The experiments were repeated three times at each heating rate to confirm the repeatability of the experiments and authenticity of the generated data (Muradov *et al.* 2010).

SEM analytical methods

The microstructure and minor element profile of the solid-state pyrolysis products were detected by SEM (JEOL JSM-6460 LV/INCA, Tokyo, Japan). The secondary electron resolution was better than 1 nm, magnification was 25 to 650,000, the imaging modes were set to secondary electron image (SEI) and back electron image (BEI), and the observed maximum height of the sample was 10 mm (Zhou and Runge 2014).

Py-GC/MS analytical methods

Analytical pyrolysis was performed using a Frontiers PY-2020is pyrolyser (Fukushima, Japan). The pyrolysis tube was successively filled with some quartz wool, 1.00 mg (0.02 mg) *Helianthus annuus* stems (Sartorius CPA225D CPA Semi-Micro Balance, Göttingen, Germany) and 1 µL ISTD. Samples were dried at room temperature under a 0.01 MPa vacuum for 10 min, and the hooks were carefully removed and placed in a thermal cracking apparatus. The pyrolysis process was carried out at the set

temperature from 300 °C to 700 °C and at the selected times of 0.1 min, 0.2 min, 0.3 min, and 0.5 min, respectively. When the conditions were available, samples were pyrolyzed according to the standard operation (Fukushima *et al.* 2009).

The pyrolysis vapors were analyzed online by GC/MS (Agilent 7890A/5975C, Santa Clara, USA). The injector temperature was kept at 290 °C. The chromatographic separation was performed using a HP-5MS capillary column (30 m × 0.25 mm i.d., 0.25 μm film thickness). Helium (99.999%) was used as a carrier gas with a constant flow rate of 1 mL/min and a 1:100 split ratio. The oven temperature was programmed from 40 °C (3 min) to 180 °C with the heating rate of 4 °C/min, then to 280 °C (4 min) with the heating rate of 10 °C/min, and then to 310 °C (4 min) with the heating rate of 10 °C/min. The temperature of the GC/MS interface was held at 280 °C, and the mass spectrometer was operated in EI mode at 70 eV. The mass spectra were obtained from m/z 20 to 400 with the scan rate of 500 Da/s and under the total ion current (TIC) mode. The chromatographic peaks were identified according to the NIST library, Wiley library, and the literature data of previous studies (Iwai *et al.* 2013). The peak of CO₂, cyclopropyl carbinol, methyl acetate, acetic acid, furan formaldehyde, 4-Hydroxy-3-methoxystyrene butane, and 3,4-dihydroxy-3-cyclobutene-1,2-dione, were confirmed through comparison with standard samples.

The ISTDs were dissolved in acetone standard solution; the final concentration was 10.0 mg/mL with 1.0 μL standard solution added in each sample. For the ISTD screening experiment, margaric acid methyl ester, nonadecane acid methyl ester, cholesterol, 1,3,5 - three tertiary butyl benzene, *etc.* were tested under pyrolysis temperature between 300 °C and 700 °C. The thermal stability, sensitivity, and linear range of the ISTDs were important factors for further research.

Qualitative and quantitative methods

For each sample, the experiments were repeated at least three times to confirm the reproducibility of the reported procedures. For each identified product, the average values of the peak area (under the TIC mode) and peak area percentage were calculated and used for analysis. In addition, the standard deviation values were also calculated.

The content determination of this experiment were divided into relative content and absolute content. The relative content referred to the material of all the percentage content of gasification product; absolute content referred to the group accounting for the proportion of the total *Helianthus annuus* stem weight. The yield of gasification production referred to the peak area of all the products divided to peak area of ISTD and then multiplied ISTD's quality.

However, the chromatographic peak area of a compound was considered to be linear with its quantity, and the peak area percentage was linear with its content. Therefore, the average peak area value obtained for each product under different reaction conditions was compared to reveal the changes of its yields, and the peak area percentage value was compared to show the change of its relative content among the detected products (Aebi *et al.* 2002).

$$\text{The yield of compositions: } W_{\text{Compositions}} = W_{\text{ISTD}} * A_{\text{Compositions}} / A_{\text{ISTD}} \quad (1)$$

$$\text{Gas yield} = A_{\text{Total}} / A_{\text{ISTD}} * W_{\text{ISTD}} \quad (2)$$

Chemometric data analysis

Data analysis was performed using SIMCAP-P V11.5 (Umetrics AB, Umea, Sweden). All processed GC/MS data were transferred to CDF file format by GC/MS ChemStation (E.02.01, Agilent Technologies), and MZmine software (2.92 <http://mzmine.github.io/>) was used to get a CVS data. Partial Least Squares Discriminant Analysis (PLS-DA), a supervised technique that facilitates classification of unknown samples against a known calibration data set, was then performed on the entire CVS data set. Discriminant analysis ($p < 0.05$) and multivariate statistical methods (Variable Importance for the Projection (VIP) > 1) selected from the vast amount of data. The statistical analysis was performed by SPSS (SPSS Inc., Chicago, USA).

RESULTS AND DISCUSSION

TG/DTA Curves of *Helianthus annuus* Stems

The thermal decomposition process of *Helianthus annuus* stems was divided into four stages (Fig. 1). The first stage was from room temperature to 150 °C, corresponding to the first peak of the DTG curve, mainly the loss physisorbed of phase *Helianthus annuus* stems, loss of crystal water occurs in the next 105 °C to 150 °C stage.

The second stage was from 160 °C to 200 °C, corresponding to the preheated solution process. At this time, the TG and DTG curves were relatively flat; primarily, the depolymerization and the "glass transition" phenomenon of small *Helianthus annuus* stems occurred (Guigo *et al.* 2010). The radical depolymerization of the stems then released a small molecule compound gas.

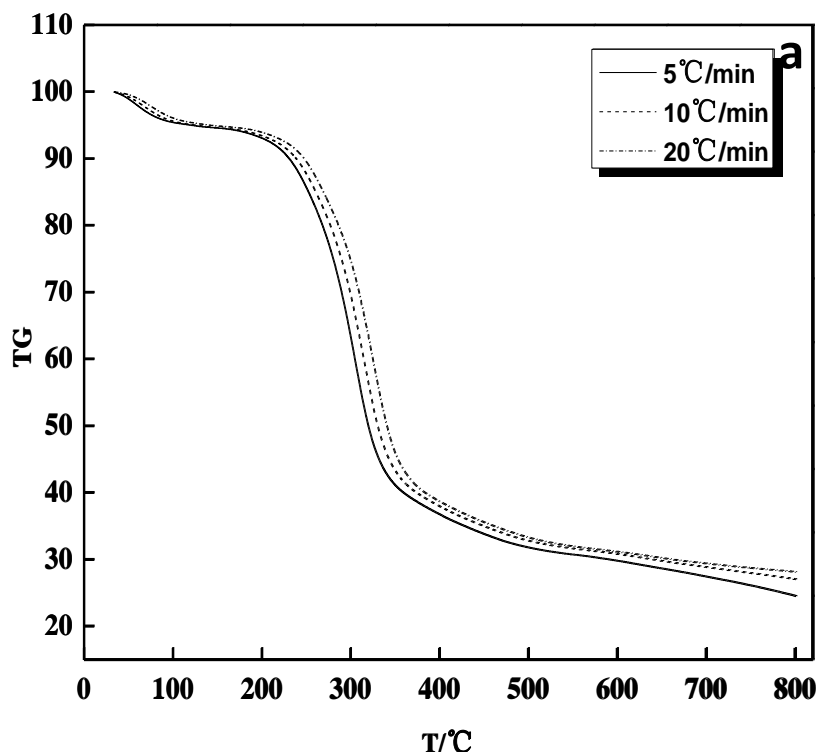


Fig. 1. (a) TG curves for *Helianthus annuus* stems at different heating rates

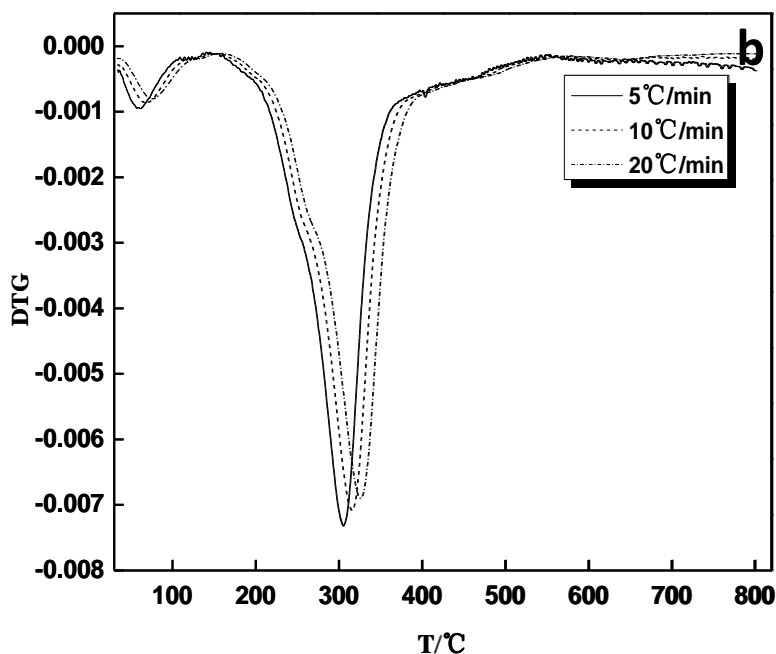


Fig. 1. (b) DTG curves for *Helianthus annuus* stems at different heating rates

The third stage was from 210 °C to 360 °C, mainly corresponding to the pyrolysis process of the *Helianthus annuus* stems. The TG curve sharply decreased. The DTG curve had two peaks. The first peak was the pyrolysis of hemicellulose and cellulose, and the second peak pyrolysis may be that of lignin (Gao *et al.* 2012). This phase pyrolyzed *Helianthus annuus* stems into numerous small and large molecules of gas condensable volatiles, resulting in a significant weight loss.

The fourth stage was from 420 °C to 800 °C, the carbonization stage of the *Helianthus annuus* stems. The pyrolysis residue underwent a slow process of carbonization, and the TG and DTG curves changed slowly also. The lignin pyrolysis temperature range of *Helianthus annuus* stems was wide, so that there was also a wide DTG curve peak. In regard to the temperature and heating rate, the TG/DTG curves provided basic pyrolysis conditions in the next PY-GC/MS experiments.

Microstructures of Solid-State Pyrolysis Products by SEM

Figure 2 shows the microstructures of the solid-state pyrolysis products prepared at different pyrolysis temperatures and time as detected by SEM. The *Helianthus annuus* stems became porous structures when heated from 300 °C to 700 °C, and the pores and mesh structure gradually increased along with the pyrolysis temperatures (Fig. 2). The porous structures were further developed as the pyrolysis time increased from 0.1 min to 0.5 min at 600 °C. However, sintering occurred, and the microporous structures were destroyed when the pyrolysis time exceeded 0.5 min (Fig. 3). These experimental results verified previous studies by Cetin *et al.* (2004). The different between Fig. 2c (700 °C, 0.2 min) and Fig. 3c (600 °C, 0.5 min) provide a reminder that pyrolysis time can have great influence than the pyrolysis temperature in the formation of pore structures generated by destroyed the microporous structures.

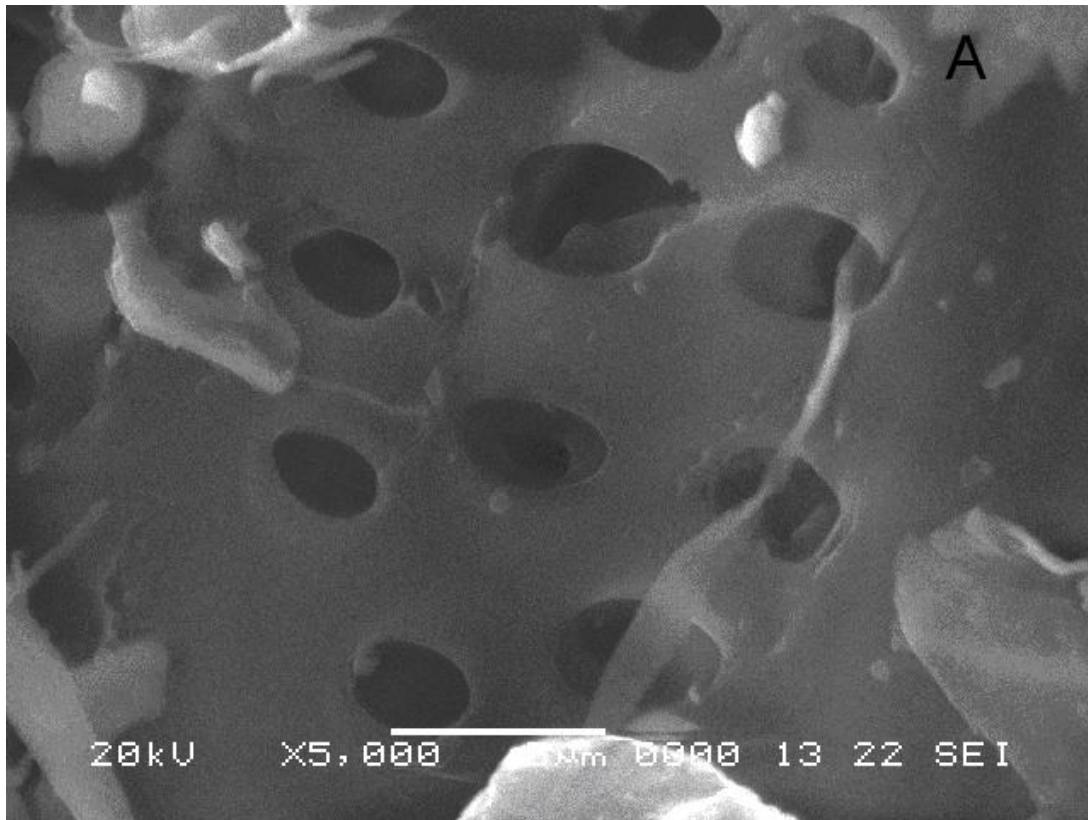


Fig. 2a. Microstructure of solid-state pyrolysis products prepared at 300 °C, 0.2 min

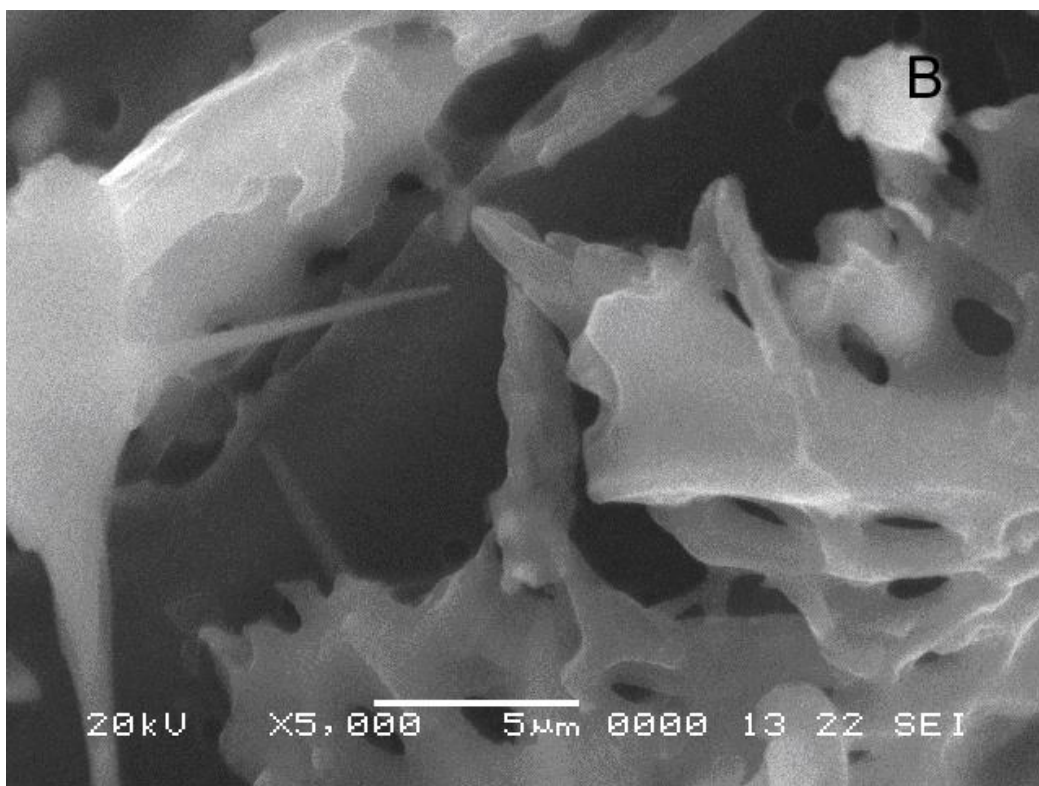


Fig. 2b. Microstructure of solid-state pyrolysis products prepared at 500 °C, 0.2 min

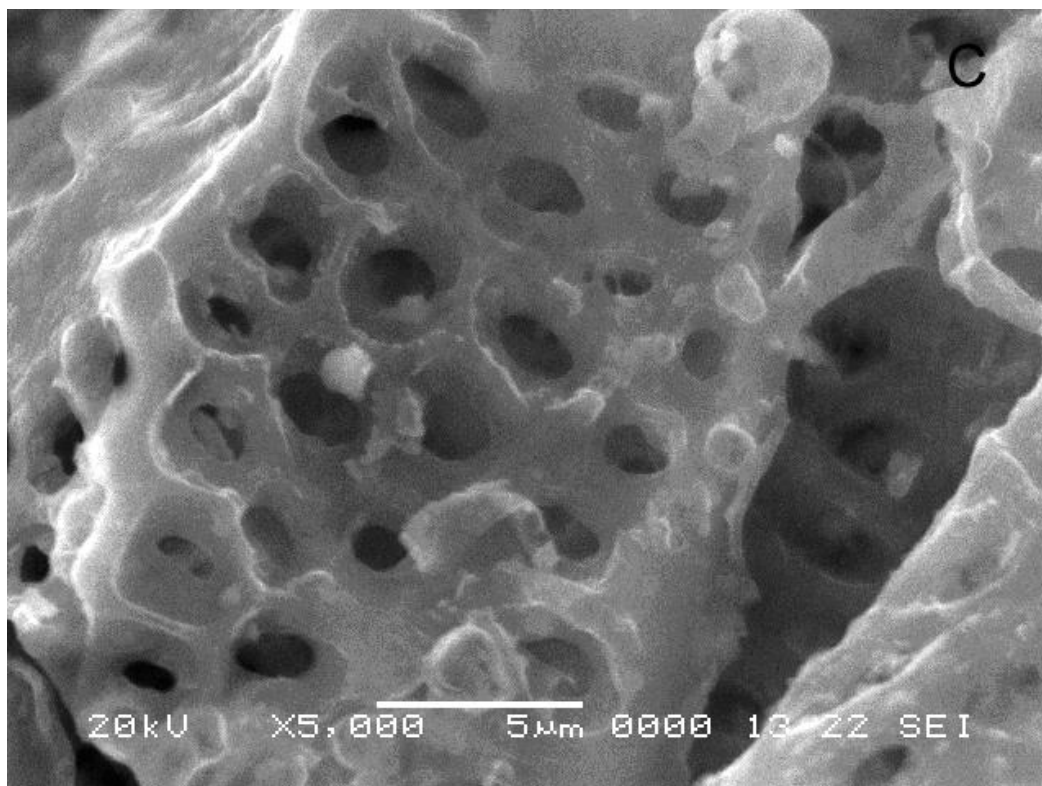


Fig. 2c. Microstructure of solid-state pyrolysis products prepared at 700 °C, 0.2 min

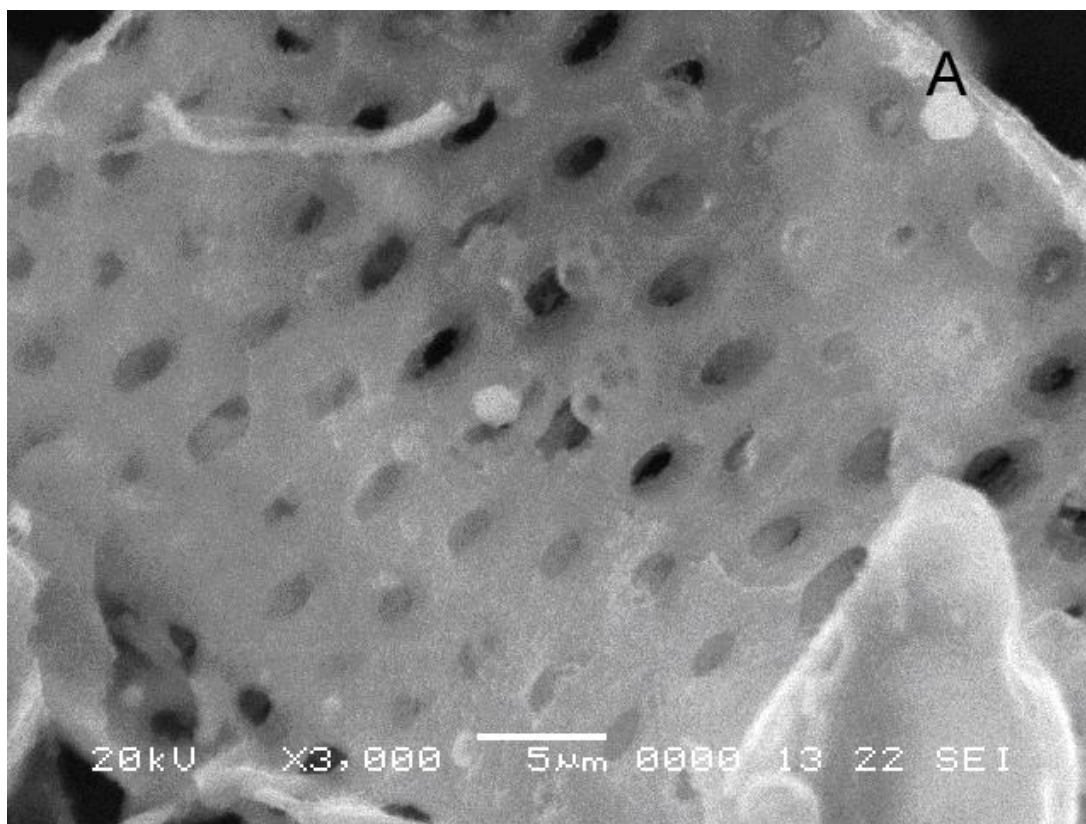


Fig. 3a. Microstructure of solid-state pyrolysis products prepared at pyrolysis times 0.1 min (600 °C)

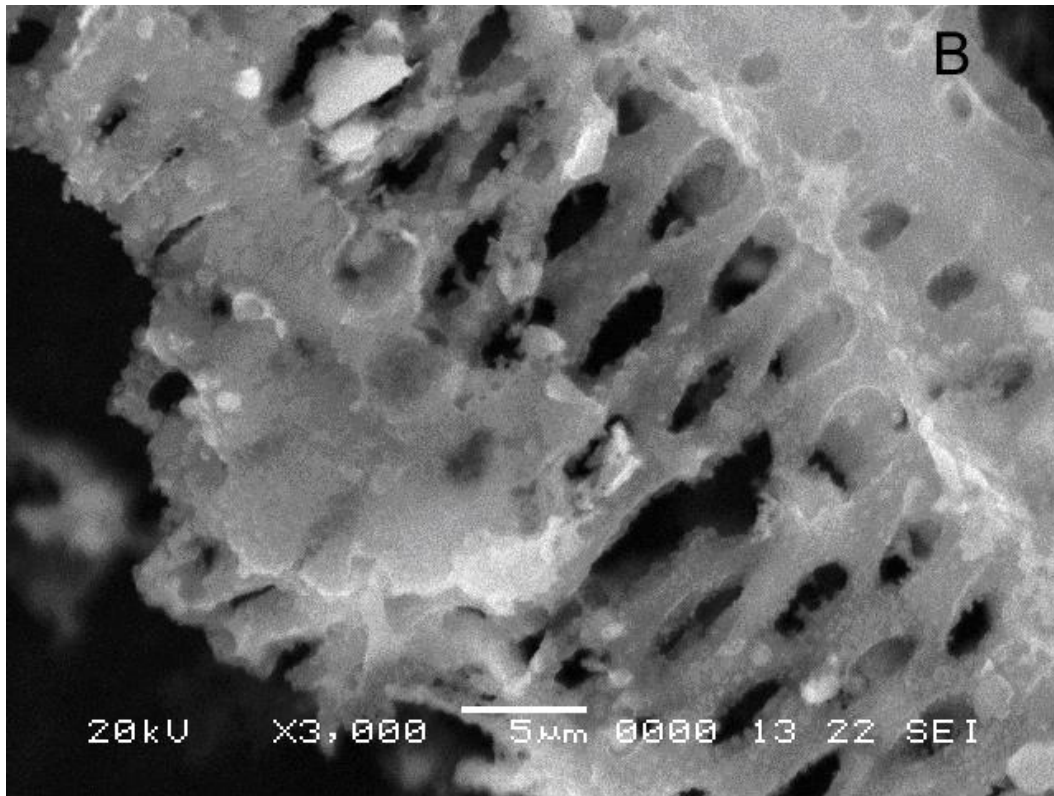


Fig. 3b. Microstructure of solid-state pyrolysis products prepared at pyrolysis times 0.2 min (600 °C)

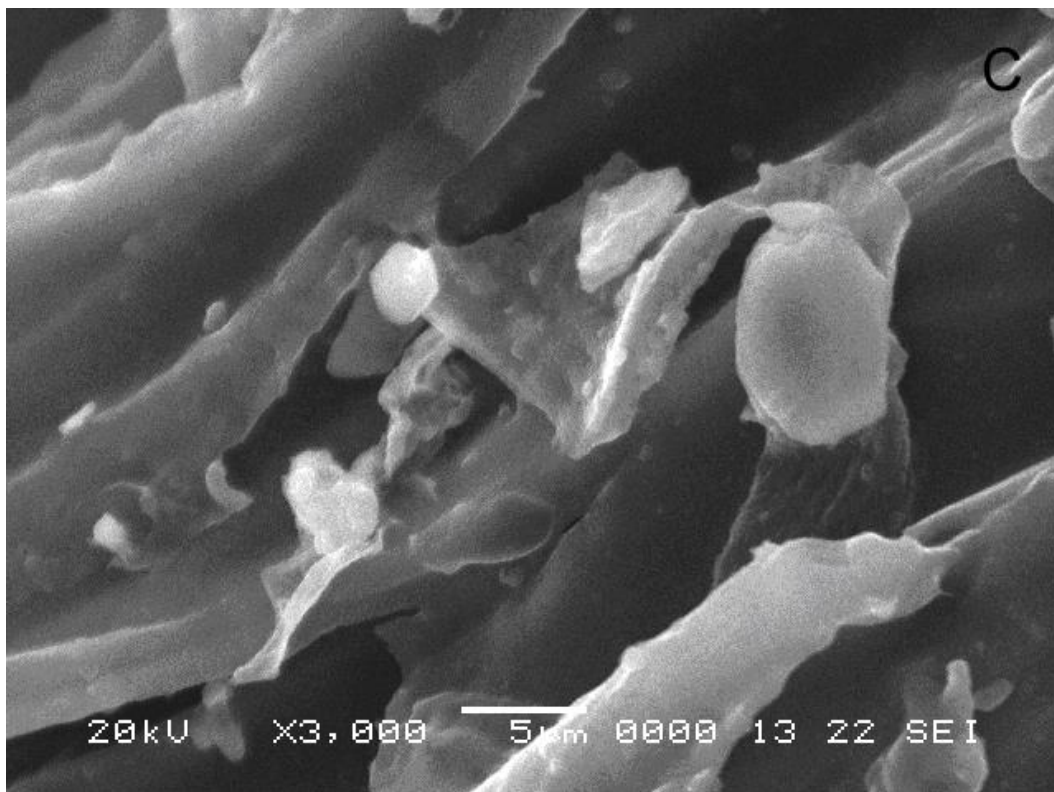


Fig. 3c. Microstructure of solid-state pyrolysis products prepared at pyrolysis times 0.5 min (600 °C)

Screening Internal Standard

In this study, margaric acid methyl ester, nonadecane acid methyl ester, 1-tridecanol, and cholesterol as common ISTDs in GC/MS were first tested under different pyrolysis temperatures and times (Razboršek 2011). They exhibited relative thermal stability at 300 °C, but they decomposed at temperatures less than 350 °C and had no obvious regularity at a higher temperature. Cholesterol is a relatively stable compound with high boiling point, but it decomposed in this experiment. Figure 4 shows the total ion chromatograms (TIC) of the pyrolysis products of cholesterol at the condition of 350 °C and 0.2 min.

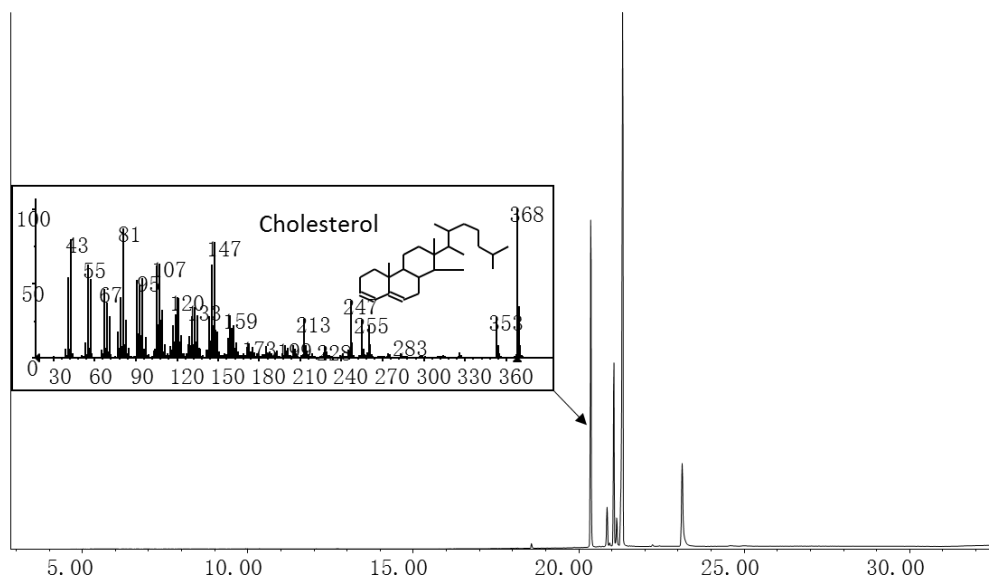


Fig. 4. Pyrolysis products of cholesterol under 350 °C at 0.2 min ($t_R = 20.338$)

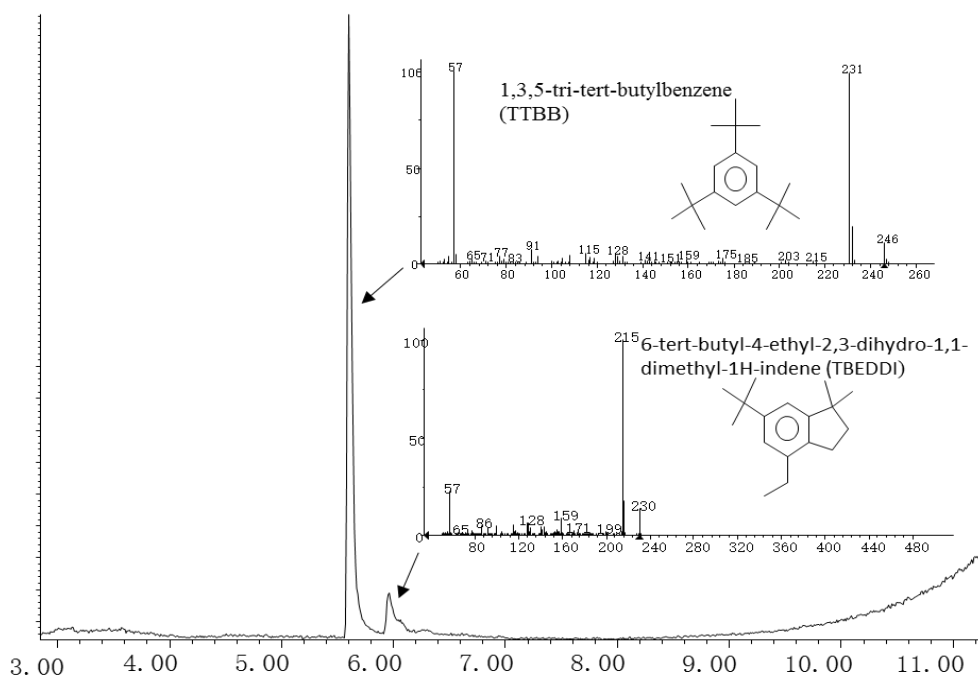


Fig. 5. Pyrolysis products of ISTD under 700 °C, 0.2 min (TTBB $t_R = 5.599$; TBEDDI $t_R = 5.966$)

After screening, 1,3,5-tri-tert-butylbenzene (TTBB, MW = 246) showed a good thermal stability below 650 °C and rearranged regularly at 700 °C. The only rearrangement product was 6-tert-butyl-4-ethyl-2,3-dihydro-1,1-dimethyl-1H-indene (TBEDDI, MW = 230) (Fig. 5), confirmed by comparing t_r and MS with a standard sample in the same conditions. In addition, the ratio of TTPP/TBEDDI remained constant. The peak area relative standard deviation (RSD) was less than 5% after the experiment was repeated five times. Hence, in this study, TTBB was the best choice as ISTD under 700 °C.

Effect of Pyrolysis Temperature and Times on Pyrolysis Vapors

In accordance with earlier published work (Keheyani 2008; Kaewpengkrow *et al.* 2014), this study explored the pyrolysis temperature ranging from 300 °C to 700 °C with the interval temperature of 50 °C, and pyrolysis times of 0.1 min, 0.2 min, 0.3 min, and 0.5 min, respectively. From TIC, the main pyrolytic products at 350 °C and 0.2 min were identified and listed in Table 1. Because the value of the peak area greatly depended on the response factor of the MS detector, the ISTD played a very important role in the quantitative analysis by GC/MS. In this study, the relative contents in pyrolysis vapors were obtained through ChemStation software and the analysis of absolute contents were conducted *via* the addition of the ISTD.

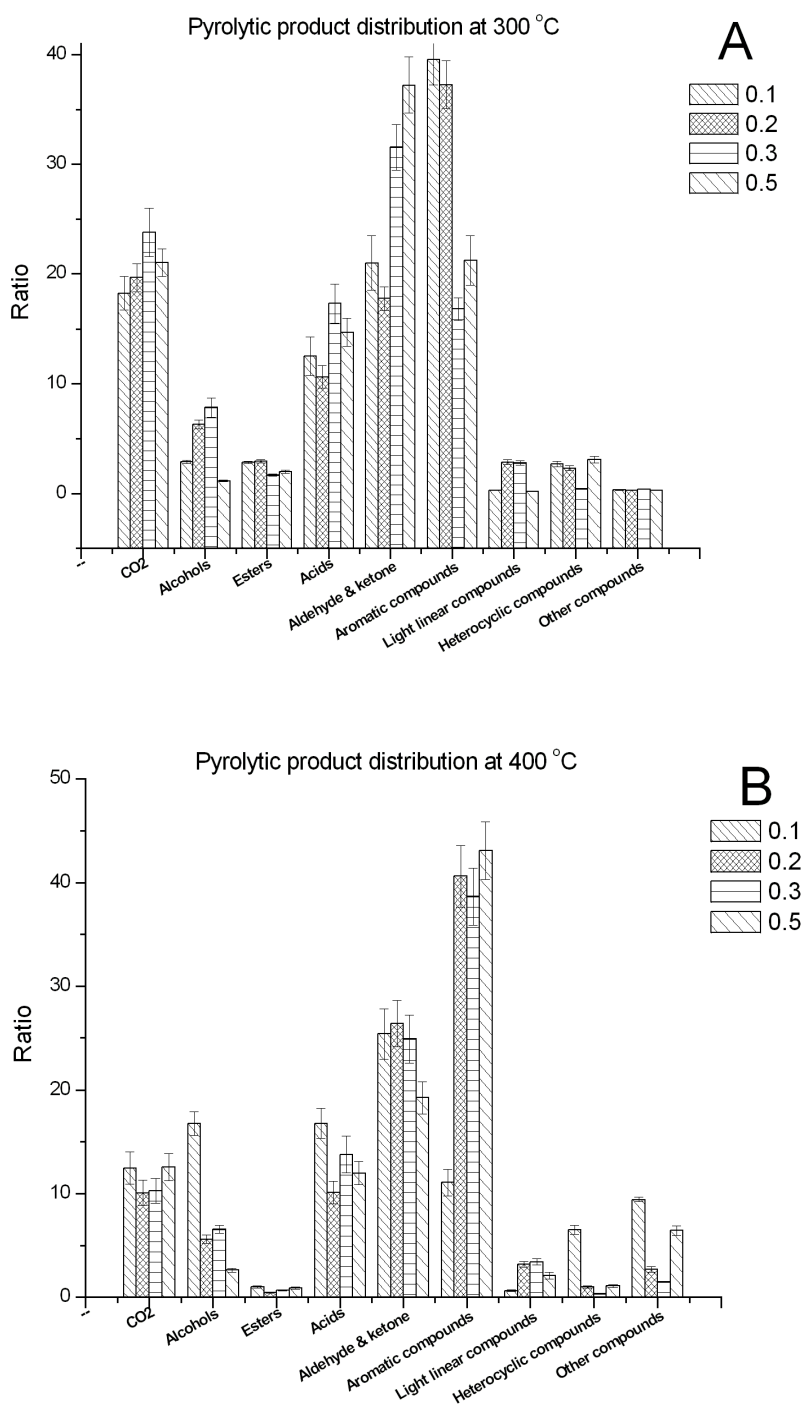
As shown in Table 2, 48 compounds were detected by GC/MS under this condition, entry 27 (RT = 27.928) was the ISTD (TTBB). In this pyrolysis process, the yield of biochemicals, CO₂, and solid-state pyrolysis products was 51%, 21.8%, and 27.2%, respectively. Alcohols, esters, acids, aldehydes, ketones, aromatic hydrocarbon, and hydrocarbon were the main biochemical products. The absolute contents of each species are also listed in Table 2.

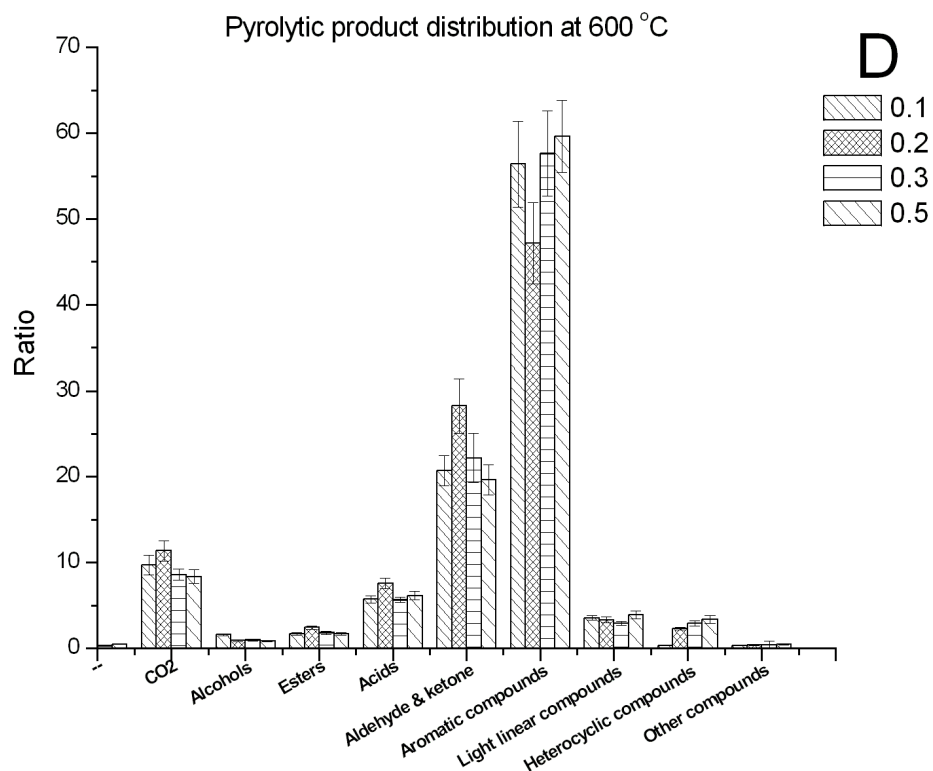
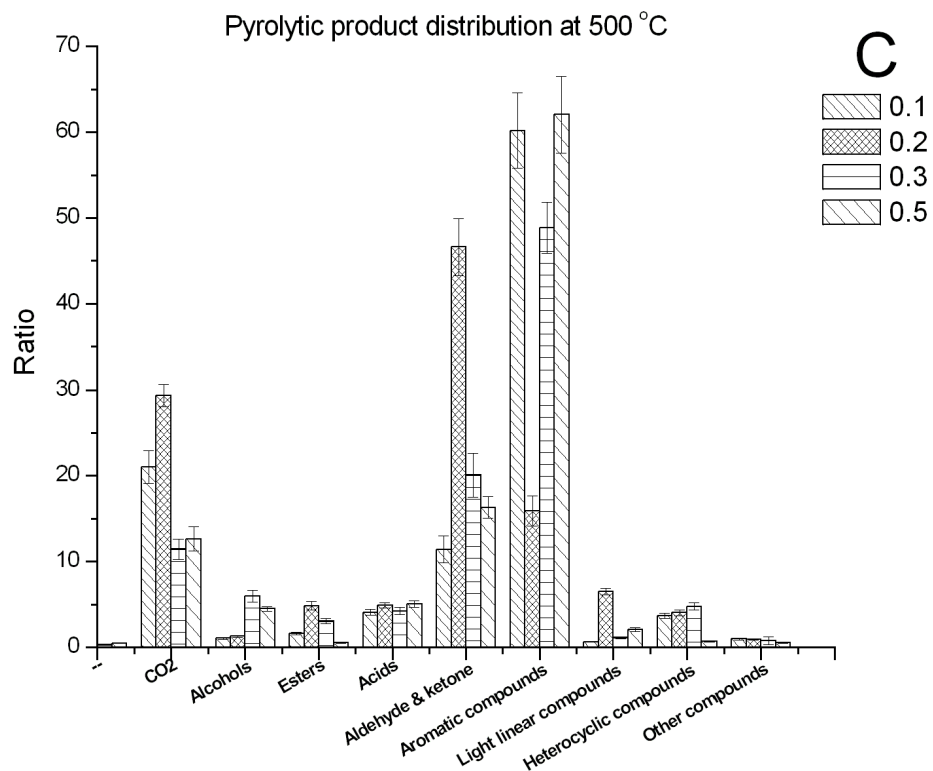
Table 2. Compounds Identified by GC/MS in the Pyrolysis Vapors of the *Helianthus annuus* Stems at 350 °C and 0.2 min

Entry	RT(min)	Compounds	Area	Relative content	Quality (mg)	Absolute content
1	1.475	Carbon dioxide	35100804	32.80%	0.21787	21.79%
2	2.501	Acetic acid	28669618	26.79%	0.177951	17.80%
3	2.852	2-Propanone, 1-hydroxy-	5926486	5.54%	0.036785	3.68%
4	3.441	Acetic acid, ethoxyhydroxy-, ethyl ester	906857	0.85%	0.005629	0.56%
5	4.527	Cyclopropyl carbinol	480844	0.45%	0.002985	0.30%
6	4.809	2-Propanone, 1-hydroxy-	1521325	1.42%	0.009443	0.94%
7	5.143	Propanal	422044	0.39%	0.00262	0.26%
8	6.631	Furfural	1615752	1.51%	0.010029	1.00%
9	7.511	Butanal	549191	0.51%	0.003409	0.34%
10	7.87	3-Aminopyrrolidine	283425	0.26%	0.001759	0.18%
11	8.426	Cyclopropyl carbinol	233005	0.22%	0.001446	0.14%
12	9.572	3-Hexene, (Z)-	853037	0.80%	0.005295	0.53%
13	9.845	2-Cyclopenten-1-one, 2-hydroxy-	3153965	2.95%	0.019577	1.96%
14	12.581	3-Cyclobutene-1,2-dione, 3,4-dihydroxy-	1307676	1.22%	0.008117	0.81%
15	13.744	2-Cyclopenten-1-one, 2-hydroxy-3-methyl-	911428	0.85%	0.005657	0.57%
16	14.436	Cycloheptanone	221344	0.21%	0.001374	0.14%
17	16.069	Phenol, 2-methoxy-	591990	0.55%	0.003674	0.37%
18	16.275	2(3H)-Furanone, dihydro-	6509102	6.08%	0.040402	4.04%

		4-hydroxy-				
19	17.198	Hydrazine, (3-fluorophenyl)-	219421	0.21%	0.001362	0.14%
20	18.651	3-Butenamide	351616	0.33%	0.002182	0.22%
21	20.823	1,2-Benzenediol	393045	0.37%	0.00244	0.24%
22	22.447	1,2-Benzenediol, 3-methoxy-	499661	0.47%	0.003101	0.31%
23	22.935	Phenol, 4-ethyl-2-methoxy-	488478	0.46%	0.003032	0.30%
24	24.106	2-Methoxy-4-vinylphenol	2351139	2.20%	0.014593	1.46%
25	25.389	Phenol, 2,6-dimethoxy-	2913893	2.72%	0.018086	1.81%
26	27.184	2-Fluoro-1,3-dimethyl-1,3,2-diazaphosphole, 2-oxide	380438	0.36%	0.002361	0.24%
27	27.928	Benzene, 1,3,5-tri-tert-butyl- (ISTD)	1611093	1.51%	0.01	1.00%
28	28.501	Phenol, 2-methoxy-4-(1-propenyl)-	1875502	1.75%	0.011641	1.16%
29	29.809	.beta.-D-Glucopyranose, 1,6-anhydro-	1789993	1.67%	0.01111	1.11%
30	30.843	Benzene, 1,2,3-trimethoxy-5-methyl-	480786	0.45%	0.002984	0.30%
31	31.057	2-Propanone, 1-(4-hydroxy-3-methoxyphenyl)-	385259	0.36%	0.002391	0.24%
32	31.989	2,3,5,6-Tetrafluoroanisole	3803546	3.55%	0.023608	2.36%
33	33.092	Phenol, 2,6-dimethoxy-4-(2-propenyl)-	227328	0.21%	0.001411	0.14%
34	34.477	Phenol, 2,6-dimethoxy-4-(2-propenyl)-	281745	0.26%	0.001749	0.17%
35	35.169	Phenethylamine, 3,4,5-trimethoxy-.alpha.-methyl-	217091	0.20%	0.001347	0.13%
36	35.845	Phenol, 2,6-dimethoxy-4-(2-propenyl)-	1720644	1.61%	0.01068	1.07%
37	37.076	4-((1E)-3-Hydroxy-1-propenyl)-2-methoxyphenol	2074067	1.94%	0.012874	1.29%
38	37.794	2-Pentanone, 1-(2,4,6-trihydroxyphenyl)	590884	0.55%	0.003668	0.37%
39	40.889	Ethyl methyl N,N-dimethylphosphoramidate	250897	0.23%	0.001557	0.16%
40	41.385	n-Hexadecanoic acid	390394	0.36%	0.002423	0.24%
41	42.018	Phenol, 2,6-dimethyl-4-nitro-	2556754	2.39%	0.01587	1.59%
42	43.693	Benzenemethanol, 3-hydroxy-.alpha.-[(methylamino)methyl]-, (R)-	181919	0.17%	0.001129	0.11%
43	48.584	Hexadecane, 2-methyl-	367178	0.34%	0.002279	0.23%
44	50.516	Heneicosane	206794	0.19%	0.001284	0.13%
45	51.115	Benzaldehyde, 4-hydroxy-, (2,4-dinitrophenyl)hydrazone	395328	0.37%	0.002454	0.25%
46	54.193	Estra-1,3,5(10)-triene-3,17-diol, 2,4-dimethoxy-, (17.beta.)-	311464	0.29%	0.001933	0.19%
47	55.065	1H-Isoindole-1,3(2H)-dione, 2-butyl-4,5,6,7-tetrahydro-	471488	0.44%	0.002927	0.29%
48	55.646	2-Ethylacridine	236430	0.22%	0.001468	0.15%
Total			117282168	100%	0.727966	72.8%

Under different pyrolysis temperatures, aldehydes, ketones, and aromatic compounds were the main products based on their higher contents (Fig. 6). For each type of compound, under different pyrolysis temperatures, a simple linear relationship between pyrolysis time and contents was not obtained. The optimal pyrolysis condition for each type of compound was different, thus providing experimental data for subsequent biochemical research and development.





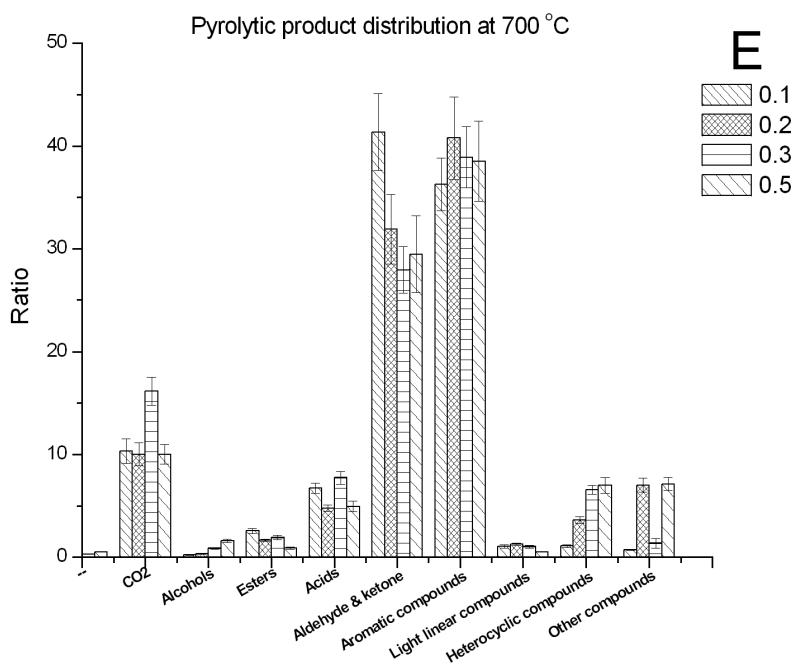


Fig. 6. Pyrolytic product distribution between 300 °C and 700 °C: (a) 300 °C, (b) 400 °C, (c) 500 °C, (d) 600 °C, (e) 700 °C

To achieve high yield for aromatic compounds, the optimal pyrolysis temperature was 600 °C. Pyrolysis times were influenced less by the yields that ranged from 51% (0.2 min) to 61% (0.5 min). Aldehyde and ketone compounds were markedly affected by the pyrolysis conditions; the condition to get the highest yield (49%) was 500 °C for 0.2 min. The content of alcohol and acid was higher (between 5% and 19%), at relatively low temperature (between 300 °C and 400 °C), and the influence of pyrolysis time was significant. Contents of ester, long chain, and heterocyclic compounds were below approximately 5%. CO₂ was the product that needed to be avoided, whose content varied greatly from 8% to 30.5%. Its lowest content (between 8% and 11%) was obtained at 600 °C under the different pyrolysis times.

Effect of Pyrolysis Conditions for Products Distribution

In order to study the pyrolysis process further, one representative compound in each class was selected for further research (Fig. 7).

CO₂ content under different pyrolysis conditions

The reduction of the amount of CO₂ was desired during the pyrolysis process. Compared with other biochemical compounds, it not only wastes carbon sources but is also a pollutant. The contents of CO₂ under different pyrolysis temperatures and time are displayed in Fig. 7a. Following the increase of the pyrolysis temperature, CO₂ content also increased, though perhaps the pyrolysis time also influenced the yield of CO₂. Generally speaking, the absolute contents of CO₂ at 0.2 min were the lowest compared with other pyrolysis times, which may be the result of a thermodynamic and kinetic process interaction (Yuan *et al.* 2011).

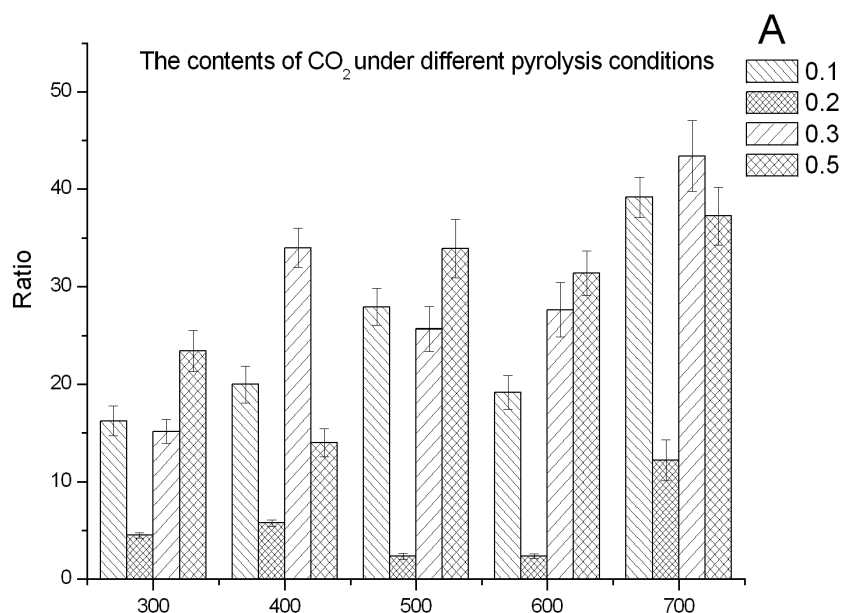


Fig. 7a. CO₂ contents under different pyrolysis temperatures (°C) and times (min)

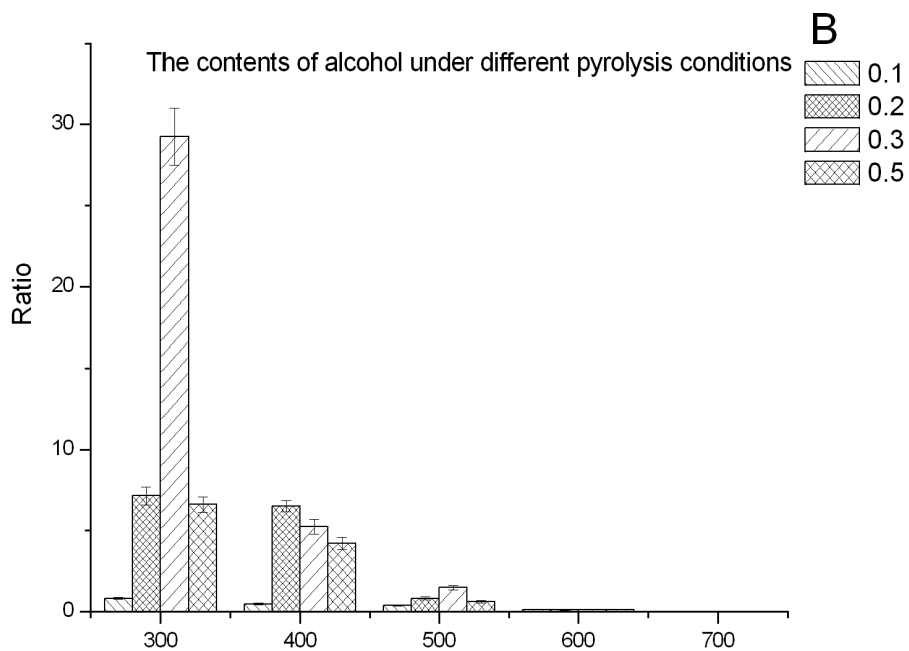


Fig. 7b. Cyclopropyl carbinol contents under different pyrolysis temperatures (°C) and times (min)

Alcohol contents under different pyrolysis conditions

In this study, the total alcohol content was relatively low; with increased pyrolysis temperature, the alcohol contents decreased. In addition, alcohol types varied according to the change in the pyrolysis temperature. In this experiment, cyclopropyl carbinol (CPMO), one of the most important alcohols in organic synthesis, was selected in order to study the pyrolysis process of alcohol. Except for at 0.5 min, the increase in the pyrolysis time resulted in elevated yields; by contrast, the increase of pyrolysis temperature was useless in improving yields (Fig. 7b). There were few CPMO produced at temperatures higher than 600 °C at any pyrolysis time. Secondary pyrolysis of alcohol at high temperature could result in the decrease of contents. As a result, 300 °C and 0.3 min were judged to be the best pyrolysis conditions for CPMO in these studies.

Ester content under different pyrolysis conditions

Methyl acetate is a commonly used chemical material and cannot be detected below 450 °C regardless of any pyrolysis temperature. The best yields were obtained when the pyrolysis temperature was increased to 500 °C (Fig. 7c). Longer pyrolysis time was not preferred in the pyrolysis of methyl acetate.

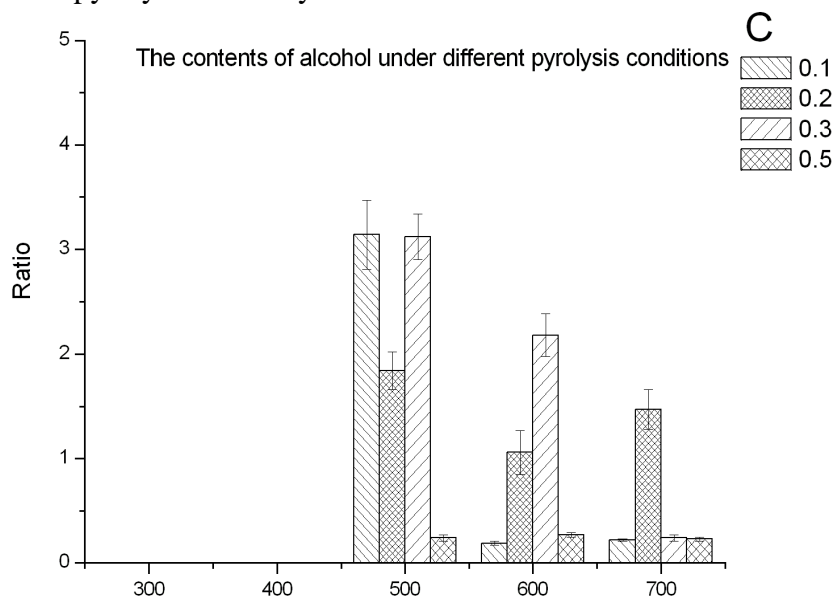


Fig. 7c. Methyl acetate contents under different pyrolysis temperatures (°C) and times (min)

Acid content under different pyrolysis conditions

Acetic acid, another important compound, showed good pyrolysis yields at 300 °C to 700 °C, as well as at 0.1 min to 0.5 min. The best yields were reached at 400 °C and at 0.2 min to 0.3 min (Fig. 7d), and similar results were obtained at other pyrolysis conditions.

Aldehyde and ketone contents under different pyrolysis conditions

Aldehyde and ketone compounds are necessary fine chemical intermediates. In this study, furan formaldehyde (FF) was chosen in order to study the pyrolysis factor for these types of compounds. Until reaching 400 °C, the biomass began to be release FF, and higher yields were achieved with higher temperature (Fig. 7e). Furan formaldehyde showed a better pyrolytic stability between 500 °C and 600 °C, where it was suitable for industrial production.

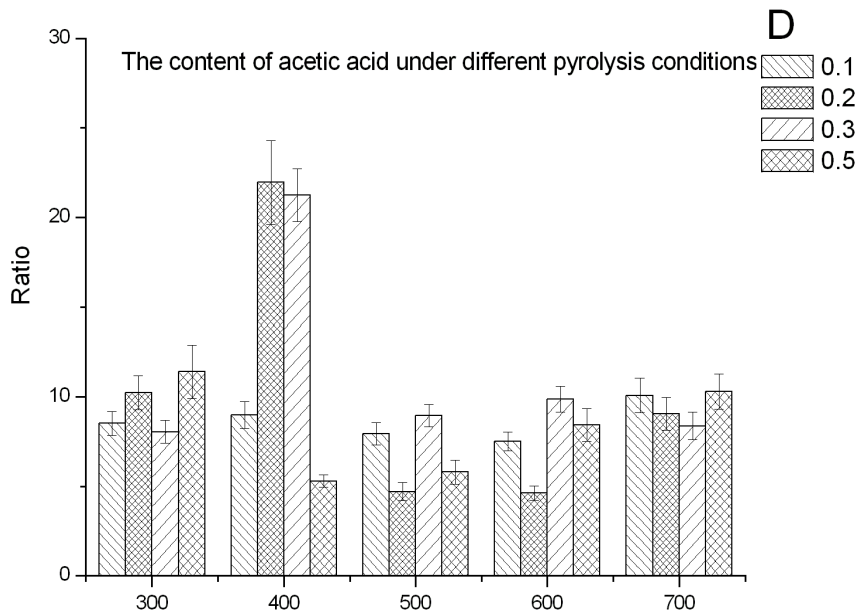


Fig. 7d. Acetic acid contents under different pyrolysis temperatures (°C) and times (min)

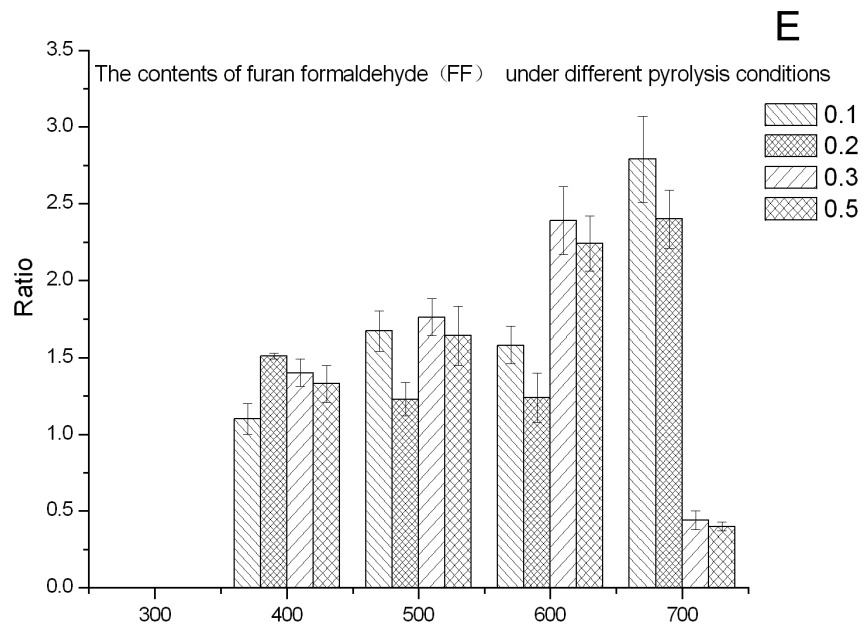


Fig. 7e. Furan formaldehyde contents under different pyrolysis temperatures (°C) and times (min)
4-Hydroxy-3-methoxystyrene content under different pyrolysis conditions

4-Hydroxy-3-methoxystyrene (HMS) is a food flavor used in many countries. As shown in Fig. 7f, higher pyrolysis temperature yielded less production of HMS, while the pyrolysis times had little effect on yield.

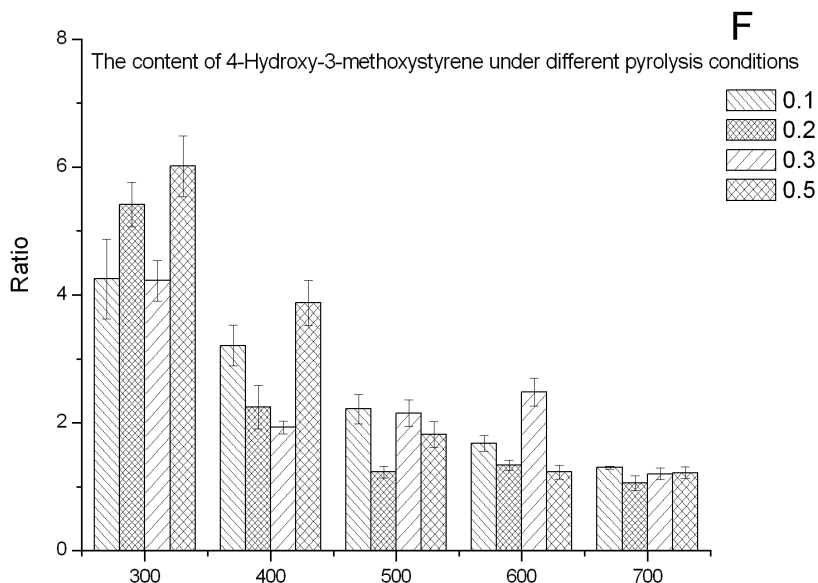


Fig. 7f. 4-Hydroxy-3-methoxystyrene contents under different pyrolysis temperatures (°C) and times (min)

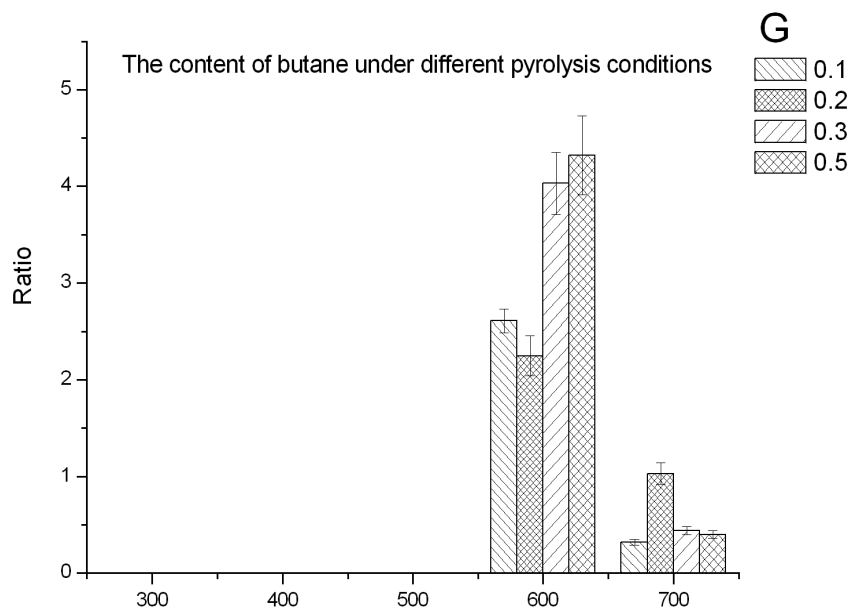


Fig. 7g. Butane contents under different pyrolysis temperatures (°C) and times (min)

Light linear compounds content under different pyrolysis conditions

Like CO₂, butane, another kind of pyrolysis gas, was only produced above 600 °C at any length of pyrolysis time (Fig. 7g). The secondary pyrolytic polymerization of pyrolysis products may have been the main cause of these small molecular alkanes.

The contents of other compounds under different pyrolysis conditions

β-D-glucopyranose, 1,6-anhydro (DGP) is a typical pyrolytic product of cellulose. It was formed through the combined intramolecular transglycosylation to form 1,6 or 1,4-anhydride, and etherification reaction to form anhydride (Fabbri *et al.* 2007). Many articles have discussed the pyrolysis mechanism about the formation of DGP. In this study, it was produced at as low as a low temperature as 300 °C (Fig. 7h).

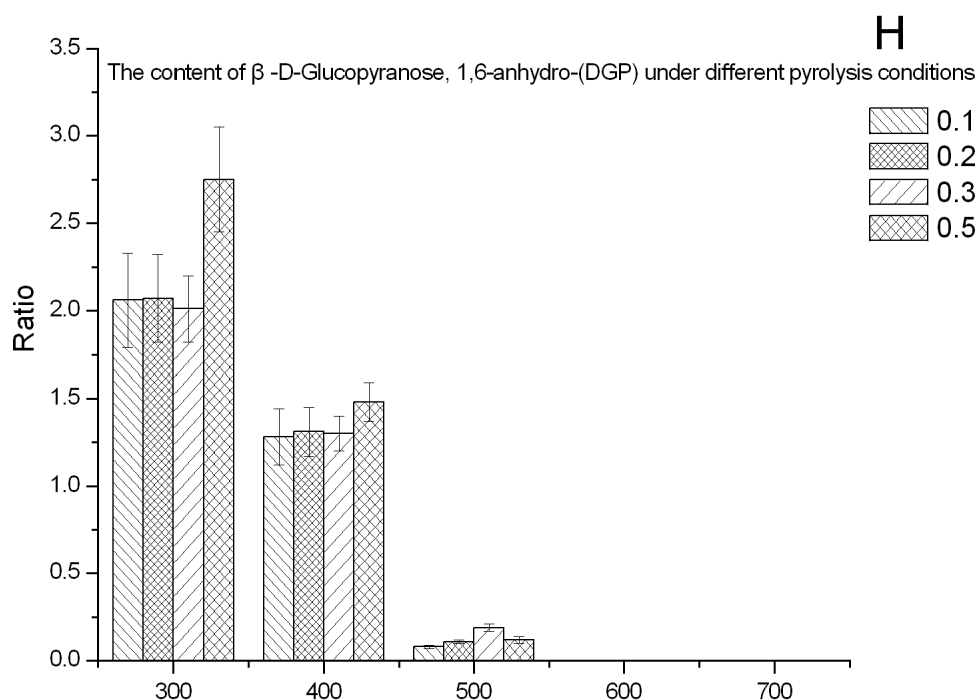


Fig. 7h. β-D-glucopyranose, 1,6-anhydro contents under different pyrolysis temperatures and times

PLS-DA Discrimination of Pyrolysis Products Difference at Unequal Temperature and Time

From the analytical data, 48 unique compounds were detected by GC/MS, and eight of them were identified compared with corresponding standard samples further (Fig. 7). Compounds were given a numerical designation. Statistical techniques were used to analyze the complex data. These methods helped to describe the observed experimental data and “find” a more efficient description of the underlying sources of sample variance (Pereira *et al.* 2010). PLS-DA was chosen as the multivariate statistical methodology (Xiang *et al.* 2011), and a series of GC/MS chromatograms were selected at a specific pyrolysis temperature (600 °C) and different pyrolysis times (0.1 min, 0.2 min, and 0.5 min) to discuss the sample difference directly (Fig. 8, n = 5).

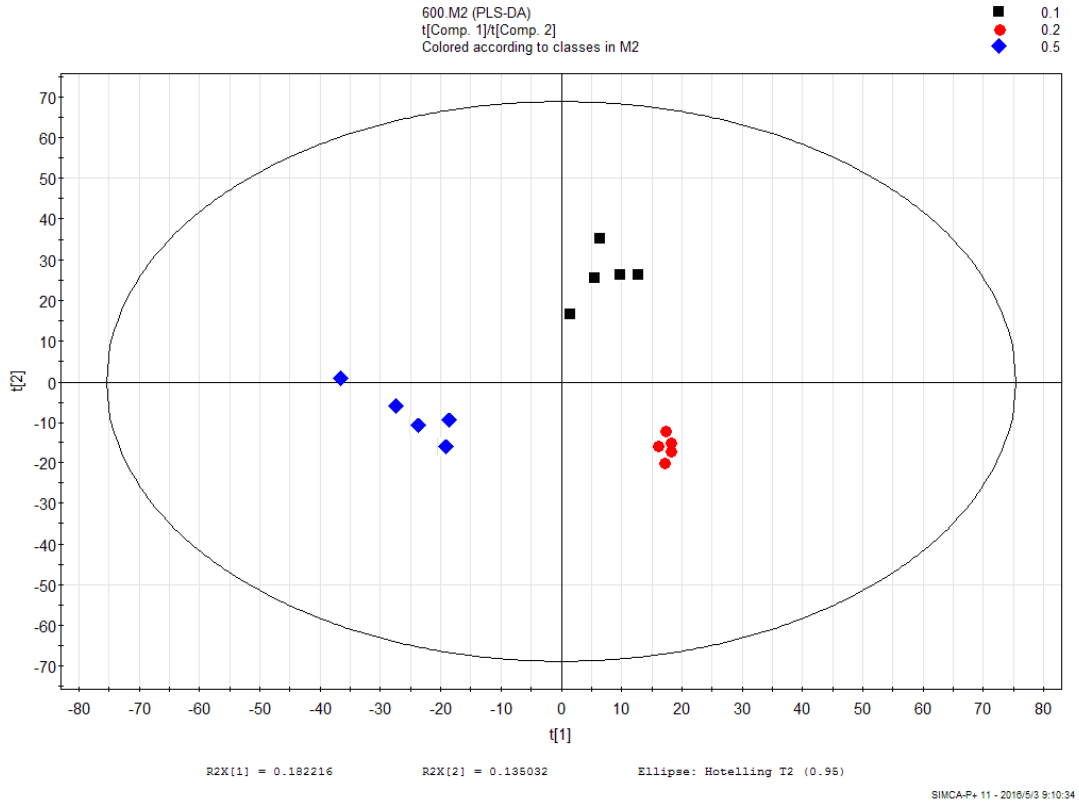


Fig. 8a. Score plot of different pyrolysis time (0.1 min, 0.2 min, and 0.5 min)

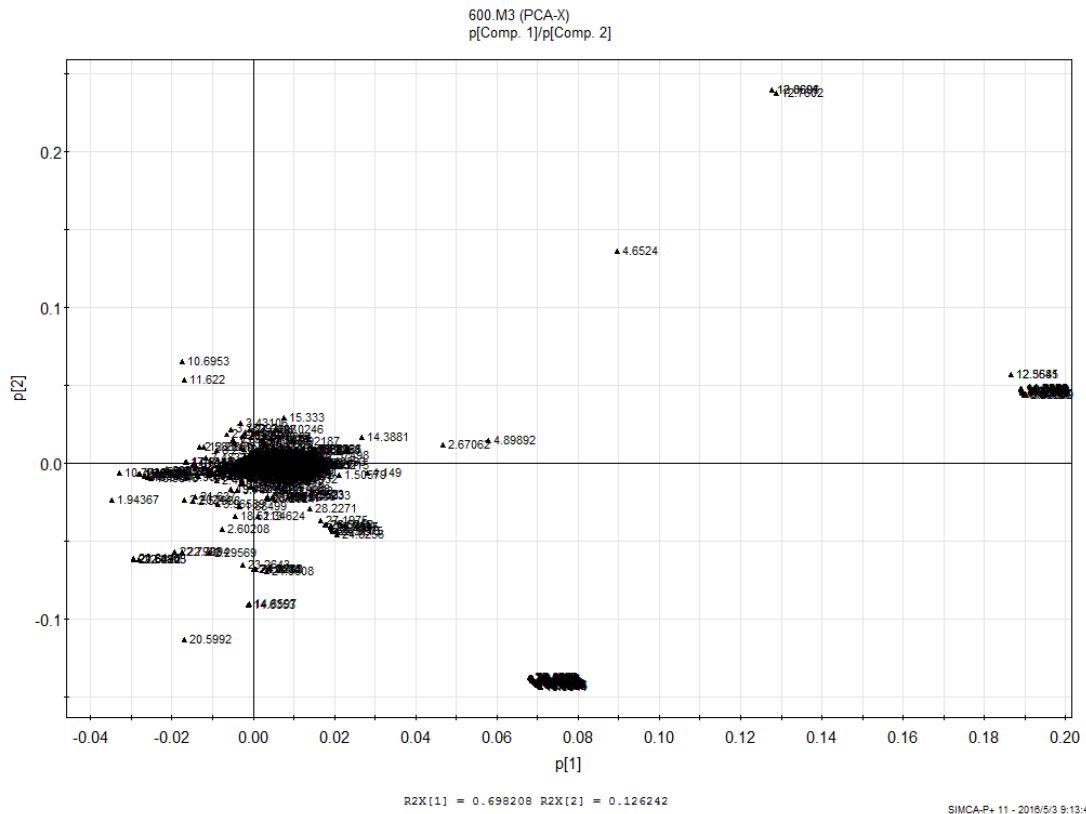


Fig. 8b. Loading plot of different pyrolysis time (0.1 min, 0.2 min, and 0.5 min)

The score plot showed that the data of the same pyrolysis time were focused in same domain and the data of different pyrolysis times were distributed in different domains. Reproducible data was relatively good, and the distance of the data points at the loading plot away from the origin reflected the degree of deviation from the PC1 (relation with retention time) and PC2 (relation with absolute content). The dot labeled as 12.5685 represents a compound that was identified by the NIST 08 database and a standard sample, 3,4-dihydroxy-3-cyclobutene-1,2-dione (Modec 2015), an important fine chemical. The corresponding dots are close to the PC1 axis and away from the PC2 axis in this condition. Thus, a small change in pyrolysis time led to great changes for this chemical. The pyrolysis time was the key factor for the oriented pyrolytic reaction.

CONCLUSIONS

1. In this study, *Helianthus annuus* stems were pyrolyzed into biochemical compounds, and the fast pyrolysis of *Helianthus annuus* stems was analyzed. The absolute contents of the product distribution affected by pyrolysis temperature and time by ISTD methods were investigated. 1,3,5-tri-tert-butylbenzene (TTBB) was the best choice of ISTD chemical under these conditions.
2. The pores and mesh structure of the solid-state pyrolysis products gradually increased along with the pyrolysis temperatures and time. Sintering and porous destruction phenomenon were observed at a lower pyrolysis temperature (600 °C) with longer time (0.5 min).
3. The content of carbon dioxide was between 8% and 30.5%, and it had to be reduced during pyrolysis. Organic volatile products were detected as qualitative and quantitative at the set pyrolysis temperature ranging from 300 °C to 700 °C. The yields of biochemicals and solid residues (except for CO₂) were approximately 51% and 27.2%, respectively, at 300 °C with 0.2 min pyrolysis time. The pyrolysis conditions for other yields were similar. When the pyrolysis temperature reached 500 °C, total absolute quality of organic compound was approximately 69%.
4. In general, the pyrolysis temperature to produce aldehydes and ketones was 700 °C, and the pyrolysis temperature to produce aromatic compounds was 600 °C. For the classification of compounds, one representative compound was chosen to summarize the rules between the product contents and pyrolysis conditions. For some pyrolysis time-sensitive compounds, such as 3,4-dihydroxy-3-cyclobutene-1,2-dione, tighter control of the pyrolysis time was important to improve its yield in the oriented pyrolytic reaction.

ACKNOWLEDGMENTS

The authors thank the National Natural Science Fund (51174279, 81402815), Major National R&D Projects (2011ZX05037-003), and the Natural Science Foundation of Shaanxi Province (No.2016JM8074) for financial support.

REFERENCES CITED

- Aebi, B., Sturny-Jungo, R., Bernhard, W., Blanke, R., and Hirsch, R. (2002). "Quantitation using GC–TOF–MS: Example of bromazepam," *Forensic Science International* 128(1-2), 84-89. DOI: 10.1016/S0379-0738(02)00165-2
- Ahmad, M., Lee, S. S., Dou, X., Mohan, D., Sung, J. K., Yang, J. E., and Ok, Y. S. (2012). "Effects of pyrolysis temperature on soybean stover- and peanut shell-derived biochar properties and TCE adsorption in water," *Bioresource Technology* 118, 536-544. DOI: 10.1016/j.biortech.2012.05.042
- Alexander, H. M., and Schrag, A. M. (2003). "Role of soil seed banks and newly dispersed seeds in population dynamics of the annual sunflower, *Helianthus annuus*," *Journal of Ecology* 91(6), 987-998. DOI: 10.1046/j.1365-2745.2003.00824.x
- Aysu, T., Maroto-Valer, M. M., and Sanna, A. (2016). "Ceria promoted deoxygenation and denitrogenation of *Thalassiosira weissflogii* and its model compounds by catalytic in-situ pyrolysis," *Bioresource Technology* 208, 140-148. DOI: 10.1016/j.biortech.2016.02.050
- Bridgwater, A. V., and Peacocke, G. V. C. (2000). "Fast pyrolysis processes for biomass," *Renewable and Sustainable Energy Reviews* 4(1), 1-73. DOI: 10.1016/S1364-0321(99)00007-6
- Butler, E., Devlin, G., Meier, D., and McDonnel, K. (2013). "Fluidised bed pyrolysis of lignocellulosic biomasses and comparison of bio-oil and micropyrolyser pyrolysate by GC/MS-FID," *Journal of Analytical and Applied Pyrolysis* 103, 96-101. DOI: 10.1016/j.jaap.2012.10.017
- Cetin, E., Moghtaderi, B., Gupta, R., and Wall, T. F. (2004). "Influence of pyrolysis conditions on the structure and gasification reactivity of biomass chars," *Fuel* 83(16), 2139-2150. DOI: 10.1016/j.fuel.2004.05.008
- Chen, Q., Zhou, J. S., Liu, B. J., Mei, Q. F., and Luo, Z. Y. (2011). "Influence of torrefaction pretreatment on biomass gasification technology," *Chinese Science Bulletin* 56(14), 1449-1456. DOI: 10.1007/s11434-010-4292-z
- Choi, M. J., and Oh, C. H. (2014). "2nd dimensional GC-MS analysis of sweat volatile organic compounds prepared by solid phase micro-extraction," *Technology and Health Care* 22(3), 481-488. DOI: 10.3233/THC-140807
- Fabbri, D., Torri, C., and Mancini, I. (2007). "Pyrolysis of cellulose catalysed by nanopowder metal oxides: production and characterisation of a chiral hydroxylactone and its role as building block," *Green Chemistry* 9(12), 1374-1379. DOI: 10.1039/B707943E
- Falco, C., Caballero, F. P., Babonneau, F., Gervais, C., Laurent, G., Titirici, M. M., and Baccile, N. (2011). "Hydrothermal carbon from biomass: Structural differences between hydrothermal and pyrolyzed carbons via ¹³C solid state NMR," *Langmuir* 27(23), 14460-14471. DOI: 10.1021/la202361p
- Fukushima, M., Yamamoto, M., Komai, T., and Yamamoto, K. (2009). "Studies of structural alterations of humic acids from conifer bark residue during composting by pyrolysis-gas chromatography/mass spectrometry using tetramethylammonium hydroxide (TMAH-py-GC/MS)," *Journal of Analytical and Applied Pyrolysis* 86(1), 200-206. DOI: 10.1016/j.jaap.2009.06.005
- Gao, A. H., Bule, M. V., Laskar, D. D., and Chen, S. (2012). "Structural and thermal characterization of wheat straw pretreated with aqueous ammonia soaking," *Journal*

- of *Agricultural and Food Chemistry* 60(35), 8632-8639. DOI: 10.1021/jf301244m
- Gopalan, N., Rodríguez-Duran, L. V., Saucedo-Castaneda, G., and Nampoothiri, K. M. (2015). "Review on technological and scientific aspects of feruloyl esterases: A versatile enzyme for biorefining of biomass," *Bioresource Technology* 193(10), 534-544. DOI: 10.1016/j.biortech.2015.06.117
- Görög, S., and Chafetz, L. (1980). "The analysis of steroids," *CRC Critical Reviews in Analytical Chemistry* 9(4), 333-383.
- Guigo, N., Mija, A., Vincent, L., and Sbirrazzuoli, N. (2010). "Eco-friendly composite resins based on renewable biomass resources: Polyfurfuryl alcohol/lignin thermosets," *European Polymer Journal* 46(5), 1016-1023. DOI: 10.1016/j.eurpolymj.2010.02.010
- Holm-Nielsen, J., and Ehimen, E. A. (2016). *Biomass Supply Chains for Bioenergy and Biorefining*, Elsevier, Amsterdam, Netherlands.
- Iwai, H., Fukushima, M., Yamamoto, M., Komai, T. and Kawabe, Y. (2013). "Characterization of seawater extractable organic matter from bark compost by TMAH-py-GC/MS," *Journal of Analytical and Applied Pyrolysis* 99, 9-15. DOI: 10.1016/j.jaap.2012.11.012
- Jabeur, H., Zribi, A., Abdelhedi, R., and Bouaziz, M. (2015). "Effect of olive storage conditions on Chemlali olive oil quality and the effective role of fatty acids alkyl esters in checking olive oils authenticity," *Food Chemistry* 169, 289-296. DOI: 10.1016/j.foodchem.2014.07.118
- Kaewpengkrow, P., Atong, D., and Sricharoenchaikul, V. (2014). "Catalytic upgrading of pyrolysis vapors from *Jatropha* wastes using alumina, zirconia and titania based catalysts," *Bioresource Technology* 163, 262-269. DOI: 10.1016/j.biortech.2014.04.035
- Keheyani, Y. (2008). "PY/GC/MS analyses of historical papers," *BioResources* 3(3), 829-837. DOI: 10.15376/biores.3.3.829-837
- Kleen, M., Lindblad, G., and Backa, S. (1993). "Quantification of lignin and carbohydrates in kraft pulps using analytical pyrolysis and multivariate data analysis," *Journal of Analytical and Applied Pyrolysis* 25, 209-227. DOI: 10.1016/0165-2370(93)80041-W
- Lu, Q., Yang, X. C., Dong, C. Q., Zhang, Z. F., Zhang, X. M., and Zhu, X. F. (2011). "Influence of pyrolysis temperature and time on the cellulose fast pyrolysis products: Analytical Py-GC/MS study," *Journal of Analytical and Applied Pyrolysis* 92(2), 430-438. DOI: 10.1016/j.jaap.2011.08.006
- Meng, H., Wang, S., Chen, L., Wu, Z., and Zhao, J. (2016). "Study on product distributions and char morphology during rapid co-pyrolysis of platanus wood and lignite in a drop tube fixed-bed reactor," *Bioresource Technology* 209, 273-281. DOI: 10.1016/j.biortech.2016.03.024
- Modéc, B. (2015). "The solid state structure of pyridinium hydrogen squarate," *Journal of Molecular Structure* 1099, 54-57. DOI: 10.1016/j.molstruc.2015.05.056
- Mohan, D., Pittman, C. U., and Steele, P. H. (2006). "Pyrolysis of wood/biomass for bio-oil: A critical review," *Energy Fuel* 20(3), 848-889. DOI: 10.1021/ef0502397
- Mullen, C. A., Boateng, A. A., Hicks, K. B., Goldberg, N. M., and Moreau, R. A. (2010). "Analysis and comparison of bio-oil produced by fast pyrolysis from three barley biomass/byproduct streams," *Energy Fuels* 24(1), 699-706. DOI: 10.1021/ef900912s
- Muradov, N., Fidalgo, B., Gujar, A. C., and Raissi, A. T. (2010). "Pyrolysis of fast-

- growing aquatic biomass—*Lemna minor* (duckweed): Characterization of pyrolysis products,” *Bioresource Technology* 101(21), 8424-8428. DOI: 10.1016/j.biortech.2010.05.089
- Naik, S., Goud, V. V., Rout, P. K., and Dalai, A. K. (2010). “Supercritical CO₂ fractionation of bio-oil produced from wheat–hemlock biomass,” *Bioresource Technology* 101(19), 7605-7613. DOI: 10.1016/j.biortech.2010.04.024
- Pereira, A. C., Reis, M. S., Saraiva, P. M., and Marques, J. C. (2010). “Analysis and assessment of Madeira wine ageing over an extended time period through GC–MS and chemometric analysis,” *Analytica Chimica Acta* 660(1-2), 8-21. DOI: 10.1016/j.aca.2009.11.009
- Razboršek, M. I. (2011). “Stability studies on *trans*-rosmarinic acid and GC–MS analysis of its degradation product,” *Journal of Pharmaceutical and Biomedical Analysis* 55(5), 1010-1016. DOI: 10.1016/j.jpba.2011.04.003
- Rostad, C. E., and Pereira, W. E. (1986). “Kovats and lee retention indices determined by gas chromatography/mass spectrometry for organic compounds of environmental interest,” *Journal of High Resolution Chromatography* 9(6), 328-334. DOI: 10.1002/jhrc.1240090603
- Shen, D. K., Gu, S., and Bridgwater, A. V. (2010). “Study on the pyrolytic behaviour of xylan-based hemicellulose using TG–FTIR and Py–GC–FTIR,” *Journal of Analytical and Applied Pyrolysis* 87(2), 199-206. DOI: 10.1016/j.jaap.2009.12.001
- Silva, R. V. S., Casilli, A., Sampaio, A. L., Ávila, B. M. F., Veloso, M. C. C., Azevedo, D. A., and Romeiro, G. A. (2014). “The analytical characterization of castor seed cake pyrolysis bio-oils by using comprehensive GC coupled to time of flight mass spectrometry,” *Journal of Analytical and Applied Pyrolysis* 106, 152-159. DOI: 10.1016/j.jaap.2014.01.013
- Sun, H., Ding, Y. Q., Duan, J. Z., Zhang, Q. J., Wang, Z. Y., Lou, H., and Zheng, X. M. (2010). “Transesterification of sunflower oil to biodiesel on ZrO₂ supported La₂O₃ catalyst,” *Bioresource Technology* 101(3), 953-958. DOI: 10.1016/j.biortech.2009.08.089
- Wang, S., Ru, B., Lin, H., Sun, W., and Luo, Z. (2015). “Pyrolysis behaviors of four lignin polymers isolated from the same pine wood,” *Bioresource Technology* 182, 120-127. DOI: 10.1016/j.biortech.2015.01.127
- Xiang, Z., Wang, X. Q., Cai, X. J., and Zeng, S. (2011). “Metabolomics study on quality control and discrimination of three *Curcuma* species based on gas chromatography-mass spectrometry,” *Phytochemical Analysis* 22(5), 411-418. DOI: 10.1002/pca.1296
- Yan, K., Liu, F., Chen, Q., Ke, M., Huang, X., Hu, W., Zhou, B., Zhang, X., and Yu, H. (2016). “Pyrolysis characteristics and kinetics of lignin derived from enzymatic hydrolysis residue of bamboo pretreated with white-rot fungus,” *Biotechnology for Biofuels* 9(76), 76-87. DOI: 10.1186/s13068-016-0489-y
- Yuan, S. A., Chen, X. L., Li, J., and Wang, F. C. (2011). “CO₂ gasification kinetics of biomass char derived from high-temperature rapid pyrolysis,” *Energy & Fuels* 25(5), 2314-2321. DOI: 10.1021/ef200051z
- Zhang, H. K., Zhou, A. N., and Chen, F. X. (2013). “Study of *helianthus annuus* stem fast pyrolysis by using Py/GC/MS,” in: *Proceedings of the 30th Annual International Pittsburgh Coal Conference*, Beijing, China, pp. 3963-3966.
- Zhang, M., Resende, F. L. P., Moutsoglou, A., and Raynie, D. E. (2012). “Pyrolysis of lignin extracted from prairie cordgrass, aspen, and kraft lignin by Py-GC/MS and

TGA/FTIR,” *Journal of Analytical and Applied Pyrolysis* 98, 65-71. DOI:

10.1016/j.jaap.2012.05.009

Zhang, S., Dong, Q., Zhang, L., and Xiong, Y. (2016). “Effects of water washing and torrefaction on the pyrolysis behavior and kinetics of rice husk through TGA and Py-GC/MS,” *Bioresource Technology* 199, 352-361. DOI:

10.1016/j.biortech.2015.08.110

Zhou, C. H., Xia, X., Lin, C. X., Tong, D. S., and Beltramini, J. (2011). “Catalytic conversion of lignocellulosic biomass to fine chemicals and fuels,” *Chemical Society Reviews* 40, 5588-5617. DOI: 10.1039/C1CS15124J

Zhou, S. F., and Runge, T. M. (2014). “Validation of lignocellulosic biomass carbohydrates determination *via* acid hydrolysis,” *Carbohydrate Polymers* 112, 179-185. DOI: 10.1016/j.carbpol.2014.05.088

Article submitted: May 24, 2016; Peer review completed: July 22, 2016; Revised version received and accepted: July 26, 2016; Published: August 25, 2016.

DOI: 10.15376/biores.11.4.8589-8614